SCIENCE CHINA
Information Sciences

• RESEARCH PAPER •

June 2018, Vol. 61 060413:1–060413:8
https://doi.org/10.1007/s11432-017-9352-0

Special Focus on Flexible Electronics Technology

# Flexible cation-based threshold selector for resistive switching memory integration

Xiaolong ZHAO[1,2], Rui WANG[2,3], Xiangheng XIAO[1*], Congyan LU[2], Facai WU[1,2], Rongrong CAO[2,3], Changzhong JIANG[1] & Qi LIU[2,3*]

[1]*Department of Physics, Hubei Nuclear Solid Physics Key Laboratory and Center for Ion beam Application, Wuhan University, Wuhan* 430072*, China;*
[2]*Key Laboratory of Microelectronic Devices & Integrated Technology, Institute of Microelectronics, Chinese Academy of Sciences, Beijing* 100029*, China;*
[3]*University of Chinese Academy of Sciences, Beijing* 100049*, China*

Received 31 October 2017/Revised 10 January 2018/Accepted 12 January 2018/Published online 18 April 2018

**Abstract** Emerging resistive switching random access memory (RRAM), considered as the most promising candidate of flash memory, is favorable for in flexible electronic system. However, in high density flexible crossbar RRAM array, crosstalk issue that currents from the neighboring unselected cell lead to failure of write and read operations, still keeps a main bottleneck. Therefore, flexible selector compatible with the flexibility of the RRAM array should be focused on to configure one selector-one resistor (1S1R) system, which is immune to crosstalk issue. In this paper, flexible cation-based threshold switching (TS) selectors (Pt/Ag/$HfO_2$/Pt/Ti/parylene) are fabricated and the compressive performance is studied systematically. The device shows excellent bidirectional volatile TS characteristics, including high selectivity ratio ($10^9$), low operating voltages ($|V_{TH}|<1$ V), ultra-low leakage current ($\sim 10^{-13}$ A) and good flexibility. The successful demonstration of the wire connected 1S1R unit comprising this flexible selector and one bipolar resistor cell indicates the great potential of this cation-based selector to restrain the crosstalk issue in a large flexible RRAM array.

**Keywords** cation-based threshold switching, resistive switching, flexible selector, conductive filament (CF), 1S1R

**Citation** Zhao X L, Wang R, Xiao X H, et al. Flexible cation-based threshold selector for resistive switching memory integration. Sci China Inf Sci, 2018, 61(6): 060413, https://doi.org/10.1007/s11432-017-9352-0

## 1 Introduction

Development of flexible electronic, wearable and implantable devices stimulates the exploration of flexible nonvolatile memory [1–4]. With the flash memory approaching its physical limit, the emerging resistive switching random access memory (RRAM) is considered as one of the most promising candidates for the next-generation nonvolatile memory [5–7]. RRAM is competitive for its two-terminal structure, simple operation, fast speed and scalable potential for 3D high-density integration [8–10], meeting the compressive requirement of this big data. Various flexible RRAM has been broadly reported, generally taking advantages of the flexibility of hybrid stacks comprising thin metal, oxide, and organics films [11–13]. However, in high density flexible crossbar RRAM array, crosstalk issue that currents from the neighboring unselected cells lead to failure of write and read operations, is still the main bottle neck problem

* Corresponding author (email: xxh@whu.edu.cn, liuqi@ime.ac.cn)

 

suppressing its practical application [14–16]. One selector-one resistor (1S1R) scheme with two-terminal selector devices have been proved the most promising way to tackle the crosstalk issue without impairing the scalability and high-density integration of the RRAM array. Selectors, such as diodes [16, 17], nonlinear devices [18, 19], volatile threshold switching (TS) devices [20, 21], have been frequently reported for 1S1R application. Generally, diodes can be utilized only for unipolar RRAM array. Though the nonlinear selectors can be developed for the most studied bipolar RRAM array, there is always a tradeoff that when larger operating voltages are used to output high selectivity (ON/OFF ratio) and ON-state current, there will be a large leakage current. By comparison, cation-based TS selectors dominated by formation/spontaneous-rupture of fragile conductive filaments (CFs) have been proved to possess low voltages, high selectivity, and ultra-low leakage current [22, 23]. Furthermore, 1S1R configuration comprising cation-based selectors functions well indicating the feasibility of future high-density integration of 1S1R RRAM array [24, 25].

Compared with the flexibility of RRAM, the flexibility of the selectors is less considered and rarely mentioned. Therefore, it is a matter of urgency to develop flexible selector to assist the application of RRAM for flexible storage. In this paper, flexible cation-based TS selectors (Pt/Ag/$HfO_2$/Pt/Ti/parylene, 5/40/20/40/5/2000 nm) with Ag as the active electrode are fabricated on $SiO_2$/Si wafer and studied systematically.

## 2 Experiments

To fabricate the device, firstly, 2 μm transparent and flexible parylene was deposited onto the clean $SiO_2$/Si wafer by thermal evaporation. Secondly, after the first ultra-violet lithography process, Pt/Ti (40/5 nm) bottom electrode (BE) was successively deposited by e-beam evaporation onto the parylene followed by a lift-off process. And then, 20 nm $HfO_2$ film was deposited by the magnetron sputtering method. Finally, after the second ultra-violet lithography process, 40 nm Ag top electrode (TE) was deposited with a 5 nm Pt coating layer, followed by a lift-off process to release the Pt/Ag/$HfO_2$/Pt/Ti/parylene devices. 4 μm×4 μm crossbar devices were electrically measured for data. Electrical characterizations were performed by Agilent B1500A semiconductor device analyzer with Pt bottom electrode grounded and Pt/Ag top electrode biased.

## 3 Results and discussions

### 3.1 Device configuration

Figure 1(a) shows the schematic illustration of the designed Pt/Ag/$HfO_2$/Pt/Ti/parylene cation-based resistive switching (RS) devices, while the SEM image of the devices is shown in Figure 1(b). Actually, the whole layers of fresh devices can be peeled off from the $SiO_2$/Si wafer owing to the weak interaction of the parylene with the wafer as shown in Figure 1(c). This makes it agile to be transferred to arbitrary substrate according to various requirement. Figure 1(d) shows the photograph of the coiled sample plying-up onto one finger, indicating its flexibility potential.

### 3.2 RS characteristics of the pristine devices on wafer

All pristine devices show high resistance state (HRS) with extremely low OFF state current ($10^{-13}$ A) under 0.2 V read bias and need an electroforming operation to initialize the subsequent RS behavior, just like most of the other RRAM devices [26, 27]. After forming to low resistance state (LRS) under 10 μA compliance current ($I_{CC}$) as shown in the left panel of Figure 2(a), the tested devices still show HRS as can be confirmed by the following positive SET sweeps (right panel), where the current starts from OFF state again regardless of the SET $I_{CC}$. This phenomenon, which could not hold its LRS after being opened up, is called volatile TS behaviors. The transformation from LRS to HRS under near-zero bias can be ascribed to the spontaneous rupture of the fragile Ag CFs. Two main behaviors

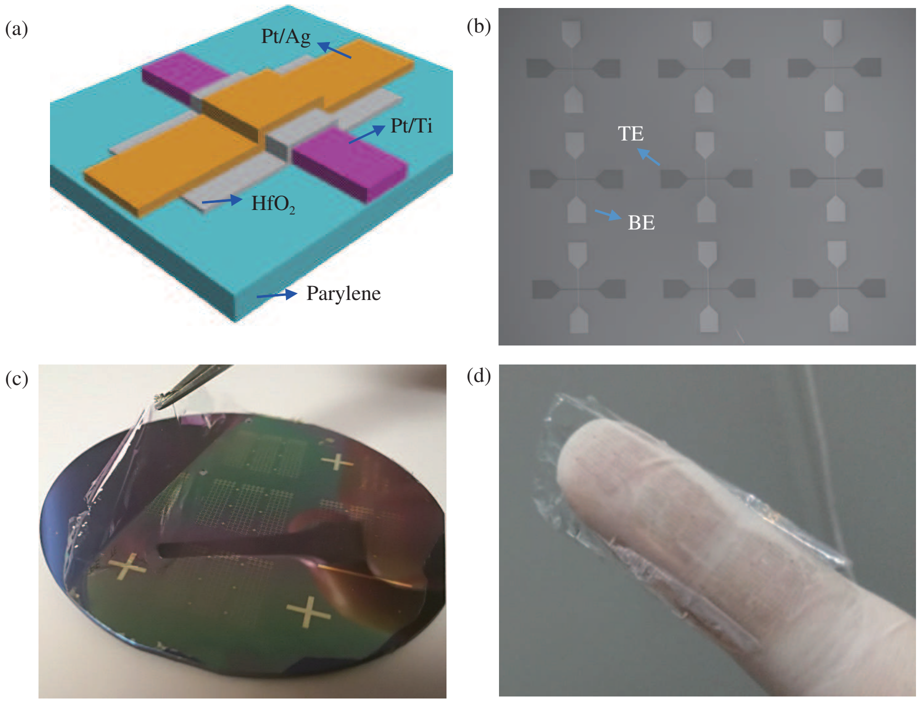


**Figure 1** (Color online) Configuration of the devices. (a) Schematic illustration of the Pt/Ag/$HfO_2$/Pt/Ti/parylene cation-based RS device; (b) SEM image of the crossbar devices; (c) peeling-off process of the fresh sample; (d) optional photograph of the coiled sample on one finger.

contribute to the spontaneous rupture of Ag CFs, (i) physical diffusion of CF component driven by the large interfacial energy [24,25], weak interaction at the CFs/$HfO_2$ interface [28] and Rayleigh instability of nanosize CFs [29,30]; (ii) electrochemical corrosion of CFs caused by nanobattery effect inside the cell [31]. Specially, this unidirectional TS behaviors can be steadily observed in the successively positive biasing sweep under 10, 50 or 100 μA $I_{\rm CC}$ after Forming operation. Unidirectional TS device is generally used to suppress the crosstalk issue in 1S1R array comprising unipolar RRAM [32]. $V_{\rm TH}$ of 200 successive positive switching cycles form three devices under 10, 50 or 100 μA $I_{\rm CC}$ respectively are shown in Figure 2(b), while the voltage distribution is shown in Figure 2(c) with the average values ($\mu$) and variance ($\delta$) of the $V_{\rm TH}$ listed at the bottom. The results show that the TS switching voltage ($V_{\rm TH}$) decreases and converges with the increment of the $I_{\rm CC}$, which can be ascribed to the difference of gap length after Ag CF rupture. With the increment of the $I_{\rm CC}$, size of the CFs increases because more Ag cation inject into the RS layer, leading to smaller gaps after CF rupture as shown in Figure 2(d), which contribute to the relative lower and concentrated switching voltages. If increasing the $I_{\rm CC}$ continuously (above 100 μA), the devices show co-existence of both volatile switching and non-volatile switching. When the $I_{\rm CC}$ is above 500 μA, the devices show stable nonvolatile RS behavior as shown in Figure 3, where LRS maintains well after removal of external bias as validated by the following read operation at 0.2 V.

It is worthy to note that the fabricated Pt/Ag/$HfO_2$/Pt/Ti/parylene cation-based RS devices can also exhibit bidirectional TS behavior, which can be utilized to tackle the crosstalk issue in most-studied bipolar RRAM array. Generally, bipolar RRAM is relatively more reliable in performance [33] and less complicated in circuitry than unipolar RRAM [34]. After forming operation, volatile TS behaviors under negative biasing sweep are also observed. Figure 4(a) shows 200 forward-backward TS switching cycles under 100 μA $I_{\rm CC}$ with $10^9$ ON/OFF ratio, while corresponding $\pm V_{\rm TH}$ ($|V_{\rm TH}|<1$ V) is shown in Figure 4(b). The penetration of Ag atoms into Pt electrode under positive sweep may form a cation source for reformation of Ag filament under negative bias [35]. Besides, motion of Ag from residual CFs is bidirectional depending on bipolar electrode effect and the electric field orientation to form continuous CFs [36,37], contributing to the bidirectional TS behavior of the device. With a 7.5 mV/step sweep rate, this selector shows sharp ~1 mV·dec$^{-1}$ turn-ON slope for both biasing polarity as shown in Figure 4(c), while the

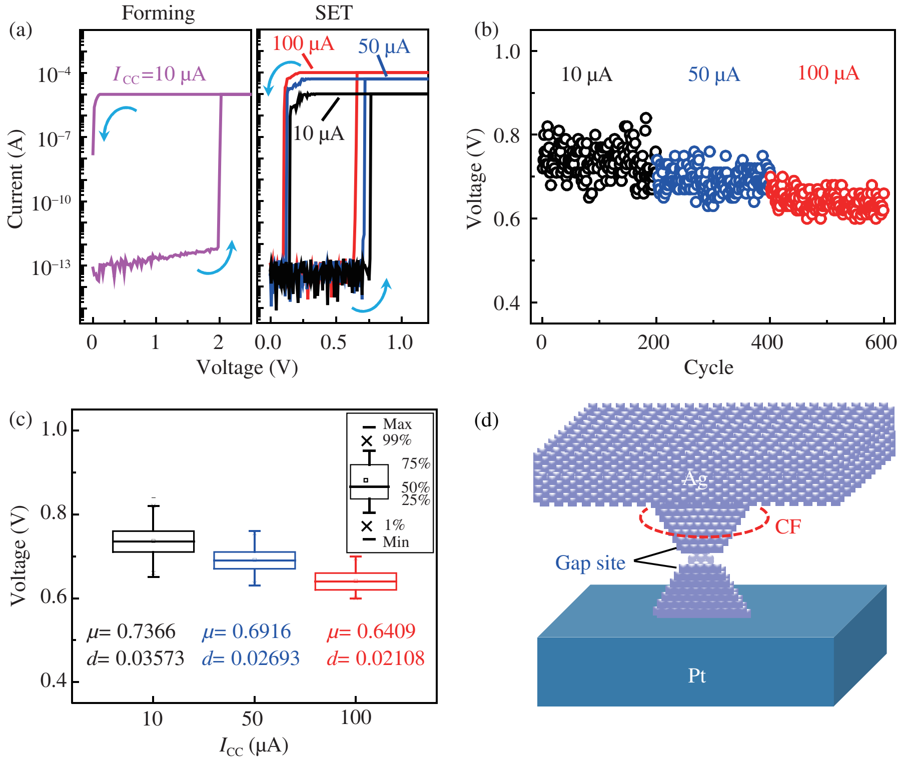


**Figure 2** (Color online) The unidirectional volatile TS behavior of the Ag/$HfO_2$/Pt/Ti/parylene devices. (a) Typical unidirectional TS I-V curves of the devices, after forming (left panel), the LRSs after SET operation (right panel) are all volatile regardless of the $I_{CC}$ (10, 50, and 100 μA); (b) $V_{TH}$ from three devices, each performed under 10, 50, and 100 μA $I_{CC}$ for 200 successive switching cycles; (c) statistical distribution of the $V_{TH}$ from (b); (d) spontaneous rupture of the fragile Ag CF under small bias generates a filament gap, while the length of the gap is strongly dependent on CF size.

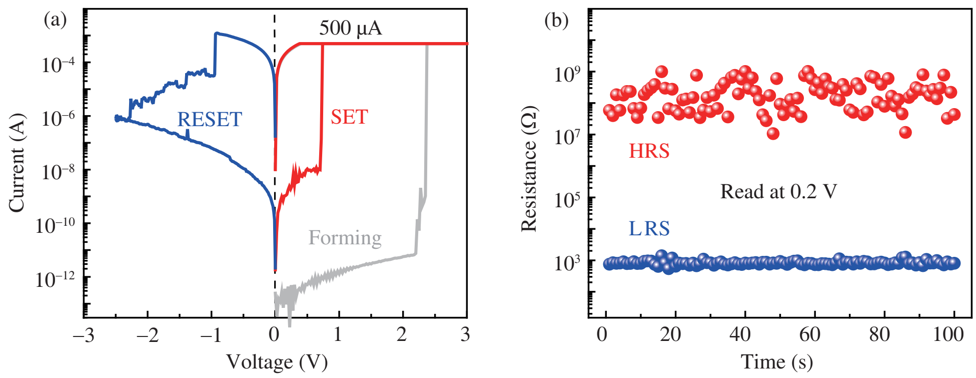


**Figure 3** (Color online) Under 500 μA $I_{CC}$, the Pt/Ag/$HfO_2$/Pt/Ti/parylene devices show stable nonvolatile RS behavior. (a) Typical I-V curves of the Pt/Ag/$HfO_2$/Pt/Ti/parylene device under 500 μA $I_{CC}$; (b) HRS and LRS (read at 0.2 V) of the device for 100 DC sweep cycles.

similar situation of the negative sweep is not shown. DC stress test of the selector in Figure 4(d) shows no obvious degradation of the device OFF state with 0.45 V bias ($V_{TH\text{-}max}/2$) for $10^4$ s at room temperature, indicating the nice stress resistance ability of the Pt/Ag/$HfO_2$/Pt/Ti/parylene cation-based selector.

### 3.3 TS characteristics of the post-coiled devices

Furthermore, the flexibility of the Pt/Ag/$HfO_2$/Pt/Ti/parylene selector is studied systematically after being peeled off from the wafer. Before measurement, the sample was coiled and flattened with a 2 mm tube in diameter for 1000 times as shown in Figure 5(a). And then the devices were tested clinging on the tube as shown in Figure 5(b). The devices still show robust endurance for more than 200 TS cycles

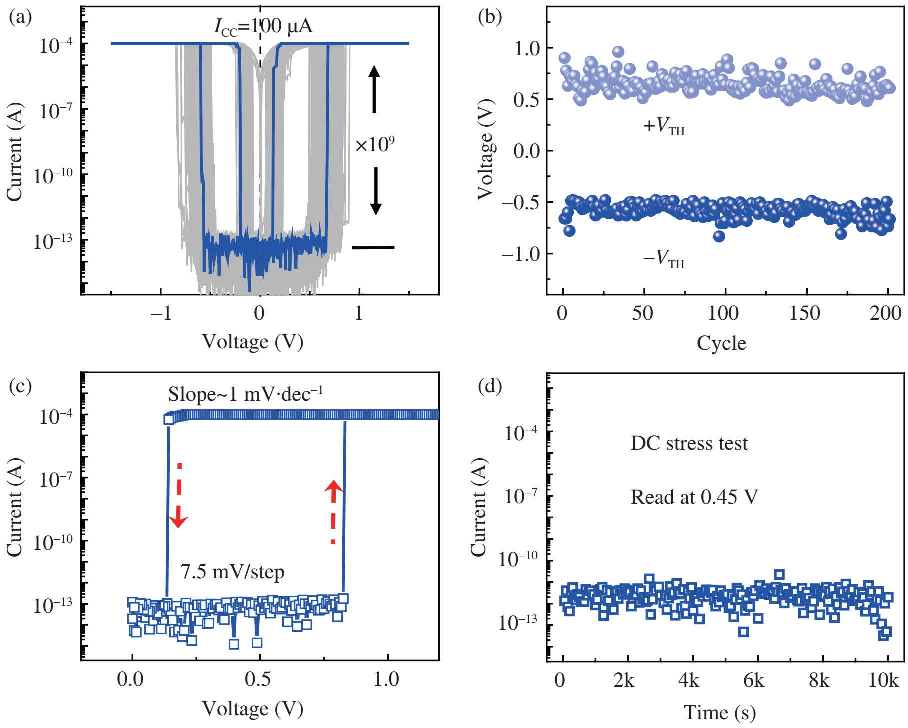


**Figure 4** (Color online) The bidirectional volatile TS behavior of the pristine Pt/Ag/$HfO_2$/Pt/Ti/parylene devices. (a) Typical bidirectional TS I-V curves of the devices under 100 μA $I_{CC}$, the LRS is volatile for both biasing polarities generating a selectivity of about $10^9$; (b) $\pm V_{TH}$ from 200 forward-backward switching cycles; (c) single positive sweep of the device with a rate of 7.5 mV·step$^{-1}$, indicating a sharp ON switching slope of about 1 mV·dec$^{-1}$; (d) DC stress test of the device at room temperature for $10^4$ s.

with high selectivity, sharp switching slope about 1 mV·dec$^{-1}$ and outstanding stress resistance ability (Figures 5(c)–(f)). All performance did not degrade obviously, indicating the excellent flexibility of the bidirectional Pt/Ag/$HfO_2$/Pt/Ti/parylene cation-based selector.

### 3.4 RS characteristics of the 1S1R unit

In order to evaluate the potential of this bidirectional Pt/Ag/$HfO_2$/Pt/Ti/parylene selector to suppress the crosstalk issue in a bipolar RRAM array, the post-coiled selector has been assembled with a Cu/$HfO_2$/Pt memory into a wire connected 1S1R unit. Figure 6(a) illustrates the typical I-V curves of the single Cu/$HfO_2$/Pt memory. As shown in Figure 6(b), during the first positive sweep "1" (0−1.5 V), the selector turns to ON-state at about 0.65 V and the memory turns to ON-state at about 1.3 V. The subsequent positive sweep "2" verifies the LRS of the memory. During the negative biasing sweep "3", the selector turns to ON-state at about −0.65 V and then the memory switches gradually back to OFF state. The following negative sweep "4" verifies the HRS of the memory. This successful write-read-erase-read cycle indicates that this bidirectional Pt/Ag/$HfO_2$/Pt/Ti/parylene flexible selector is able to restrain the crosstalk issue in a large memory array.

## 4 Summary

In summary, Pt/Ag/$HfO_2$/Pt/Ti/parylene flexible cation-based TS selectors were fabricated and studied systematically. The spontaneous rupture of the fragile Ag filaments with large interfacial energy contributes to the volatile property of the device. This selector shows excellent flexibility together with bidirectional selectivity, high selectivity ratio ($10^9$), low voltages ($|V_{TH}|$<1 V) and ultra-low leakage current (~$10^{-13}$ A), sharp switching slope (~1 mV·dec$^{-1}$) and outstanding stress resistance ability (>$10^4$ s). Furthermore, the wire connected 1S1R unit comprising this flexible selector and one bipolar

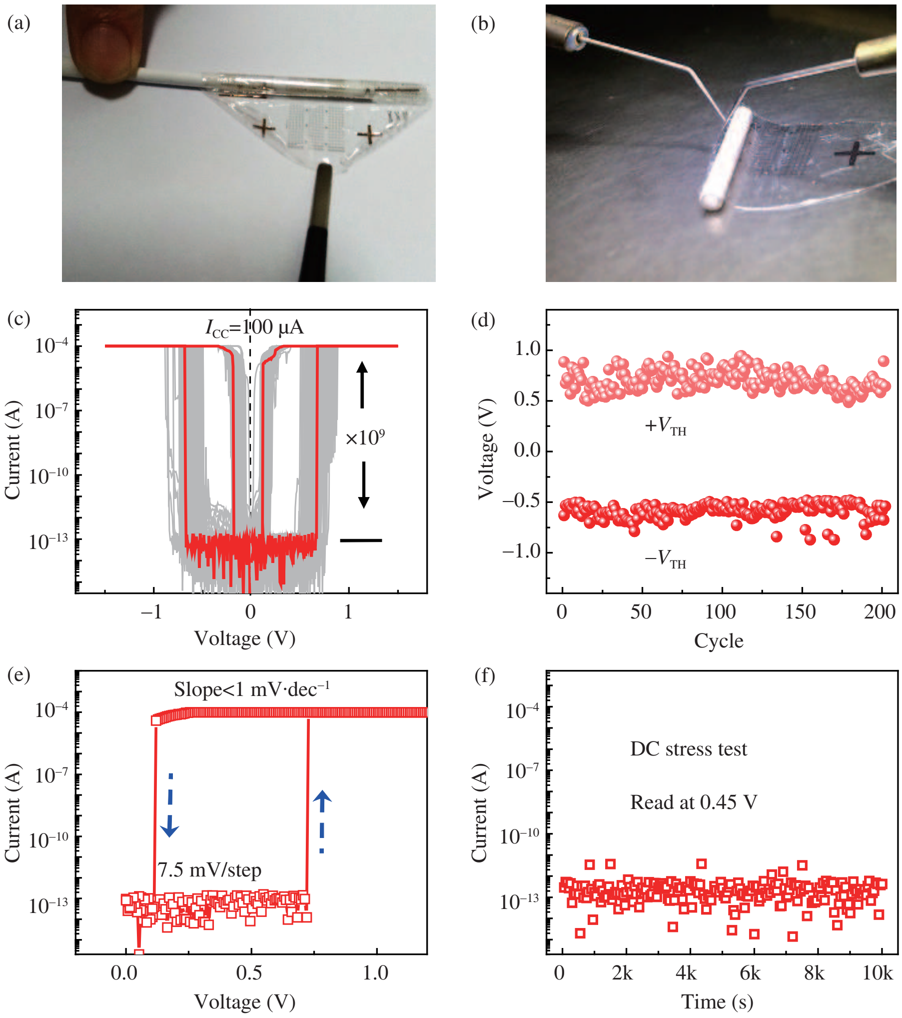


**Figure 5** (Color online) Coil measurement of the bidirectional Pt/Ag/$HfO_2$/Pt/Ti/parylene selector. (a) Optional photograph of the coiled sample on a tube with 0.2 mm diameter; (b) photograph of the test situation on the probe station; (c) I-V curves of 200 switching cycles of the coiled TS selector after being coiled and stretched for 1000 times on the tube; (d) $\pm V_{TH}$ of the 200 forward-backward switching cycles in (c); (e) sharp ON switching slope of about 1 mV·dec$^{-1}$ can also be observed after coiled; (f) the coiled selector still shows nice DC stress tolerance for $10^4$ s.

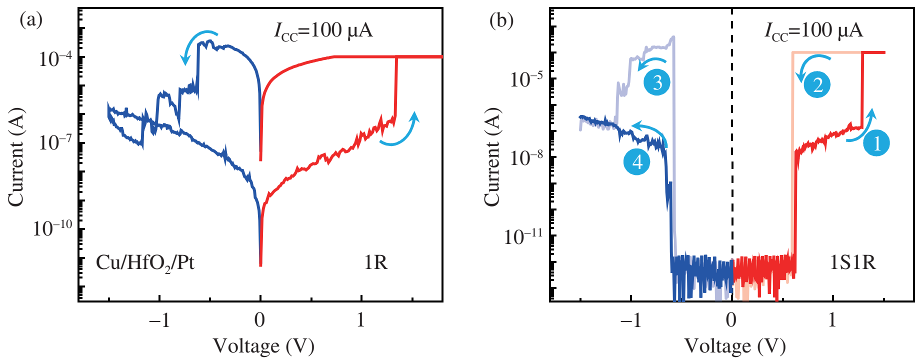


**Figure 6** (Color online) Measurement of the wire-connected 1S1R unit. (a) The typical I-V curves of the Cu/$HfO_2$/Pt device; (b) I-V curves of the Cu/$HfO_2$/Pt memory in series with the Pt/Ag/$HfO_2$/Pt/Ti/parylene cation-based selector under 100 μA $I_{CC}$.

Cu/$HfO_2$/Pt resistor functions well. The results demonstrate the great potential of this cation-based Pt/Ag/$HfO_2$/Pt/Ti/parylene selector to be applied in high density flexible crossbar RRAM array for flexible electronic, wearable and implantable systems.

**Acknowledgements** This work was supported by National Key R&D Program (Grant No. 2017YFB0405603), Beijing Training Project for the Leading Talents in S&T (Grant No. ljrc201508), Youth Innovation Promotion Association, Chinese Academy of Sciences (Grant No. 2015096), Opening Project of Key Laboratory of Microelectronics Devices and Integrated Technology, Institute of Microelectronics, Chinese Academy of Sciences (Grant No. Y7YS033003).

## References


1 Son D, Lee J, Qiao S T, et al. Multifunctional wearable devices for diagnosis and therapy of movement disorders. Nat Nanotech, 2014, 9: 397–404

2 Jo A, Seo Y, Ko M, et al. Textile resistance switching memory for fabric electronics. Adv Funct Mater, 2017, 27: 1605593

3 Choi S, Lee H, Ghaffari R, et al. Recent advances in flexible and stretchable bio-electronic devices integrated with nanomaterials. Adv Mater, 2016, 28: 4203–4218

4 Zhu B W, Wang H, Leow W R, et al. Silk fibroin for flexible electronic devices. Adv Mater, 2016, 28: 4250–4265

5 Shulaker M M, Hills G, Park R S, et al. Three-dimensional integration of nanotechnologies for computing and data storage on a single chip. Nature, 2017, 547: 74–78

6 Kim G H, Ju H, Yang M K, et al. Four-bits-per-cell operation in an $HfO_2$-based resistive switching device. Small, 2017, 13: 1701781

7 Hou Y, Chen B, Chen Z, et al. Doping profile modification approach of the optimization of $HfO_x$ based resistive switching device by inserting $AlO_x$ layer. Sci China Inf Sci, 2015, 58: 062402

8 Choi B J, Torrezan A C, Strachan J P, et al. High-speed and low-energy nitride memristors. Adv Funct Mater, 2016, 26: 5290–5296

9 Luo Q, Xu X X, Liu H T, et al. Super non-linear RRAM with ultra-low power for 3D vertical nano-crossbar arrays. Nanoscale, 2016, 8: 15629–15636

10 Wang G M, Long S B, Zhang M Y, et al. Operation methods of resistive random access memory. Sci China Technol Sci, 2014, 57: 2295–2304

11 Yang Y X, Yuan G L, Yan Z B, et al. Flexible, semitransparent, and inorganic resistive memory based on BaTi0.95Co0.05O3 film. Adv Mater, 2017, 29: 1700425

12 Shang J, Xue W H, Ji Z H, et al. Highly flexible resistive switching memory based on amorphous-nanocrystalline hafnium oxide films. Nanoscale, 2017, 9: 7037–7046

13 Yan X B, Zhou Z Y, Zhao J H, et al. Flexible memristors as electronic synapses for neuro-inspired computation based on scotch tape-exfoliated mica substrates. Nano Res, 2018, 11: 1183–1192

14 Hudec B, Hsu C W, Wang I T, et al. 3D resistive RAM cell design for high-density storage class memory-a review. Sci China Inf Sci, 2016, 59: 061403

15 Kim S, Son J H, Lee S H, et al. Flexible crossbar-structured resistive memory arrays on plastic substrates via inorganic-based laser lift-off. Adv Mater, 2014, 26: 7480–7487

16 Yoo H G, Kim S, Lee K J. Flexible one diode-one resistor resistive switching memory arrays on plastic substrates. Rsc Adv, 2014, 4: 20017–20023

17 Lo C L, Chen M C, Huang J J, et al. On the potential of CRS, 1D1R, and 1S1R crossbar RRAM for storage-class memory. In: Proceedings of IEEE Symposium on VLSI Technology, Hsinchu, 2013

18 Luo Q, Xu X X, Lv H B, et al. Fully BEOL compatible $TaO_x$-based selector with high uniformity and robust performance. In: Proceedings of IEEE International Electron Devices Meeting, San Francisco, 2016

19 Choi B J, Zhang J, Norris K, et al. Trilayer tunnel selectors for memristor memory cells. Adv Mater, 2016, 28: 356–362

20 Park J, Cha E, Karpov I, et al. Dynamics of electroforming and electrically driven insulator-metal transition in $NbO_x$ selector. Appl Phys Lett, 2016, 108: 232101

21 Jo S H, Kumar T, Narayanan S, et al. Cross-point resistive RAM based on field-assisted superlinear threshold selector. IEEE Trans Electron Devices, 2015, 62: 3477–3481

22 Bricalli A, Ambrosi E, Laudato M, et al. $SiO_x$-based resistive switching memory (RRAM) for crossbar storage/select elements with high on/off ratio. In: Proceedings of IEEE International Electron Devices Meeting, San Francisco, 2016

23 Shukla N, Grisafe B, Ghosh R K, et al. Ag/$HfO_2$ based threshold switch with extreme non-linearity for unipolar cross-point memory and steep-slope phase-FETs. In: Proceedings of IEEE International Electron Devices Meeting, San Francisco, 2016

24 Yoon J H, Zhang J M, Ren X C, et al. Truly electroforming-free and low-energy memristors with preconditioned conductive tunneling paths. Adv Funct Mater, 2017, 27: 1702010

25 Midya R, Wang Z R, Zhang J M, et al. Anatomy of Ag/Hafnia-based selectors with 1010 nonlinearity. Adv Mater, 2017, 29: 1604457

26 Hui F, Grustan-Gutierrez E, Long S B, et al. Graphene and related materials for resistive random access memories. Adv Electron Mater, 2017, 3: 1600195

27 Zhao X L, Liu S, Niu J B, et al. Confining cation injection to enhance CBRAM performance by nanopore graphene

layer. Small, 2017, 13: 1603948
28 Cho D Y, Tappertzhofen S, Waser R, et al. Bond nature of active metal ions in $SiO_2$-based electrochemical metallization memory cells. Nanoscale, 2013, 5: 1781–1784
29 Volk A, Knez D, Thaler P, et al. Thermal instabilities and Rayleigh breakup of ultrathin silver nanowires grown in helium nanodroplets. Phys Chem Chem Phys, 2015, 17: 24570–24575
30 Hsiung C P, Liao H W, Gan J Y, et al. Formation and instability of silver nanofilament in Ag-based programmable metallization cells. ACS Nano, 2010, 4: 5414–5420
31 Tappertzhofen S, Linn E, Bottger U, et al. Nanobattery effect in RRAMs-implications on device stability and endurance. IEEE Electron Device Lett, 2014, 35: 208–210
32 Song J, Woo J, Yoo J, et al. Effects of liner thickness on the reliability of AgTe/$TiO_2$-based threshold switching devices. IEEE Trans Electron Device, 2017, 64: 4763–4767
33 Tran X A, Zhu W, Liu W J, et al. A self-rectifying $AlO_y$ bipolar RRAM with Sub-50-μA set/reset current for cross-bar architecture. IEEE Electron Device Lett, 2012, 33: 1402–1404
34 Wong H S P, Lee H Y, Yu S, et al. Metal-oxide RRAM. Proc IEEE, 2012, 100: 1951–1970
35 Liu S, Lu N D, Zhao X L, et al. Eliminating negative-SET behavior by suppressing nanofilament overgrowth in cation-based memory. Adv Mater, 2016, 28: 10623–10629
36 Yang Y C, Gao P, Li L Z, et al. Electrochemical dynamics of nanoscale metallic inclusions in dielectrics. Nat Commun, 2014, 5: 4232
37 Song J, Prakash A, Lee D, et al. Bidirectional threshold switching in engineered multilayer ($Cu_2O$/Ag:$Cu_2O$/$Cu_2O$) stack for cross-point selector application. Appl Phys Lett, 2015, 107: 113504